Phase explosion in atmospheric pressure infrared laser ablation from water-rich targets

Zhaoyang Chen
Department of Chemistry, The George Washington University, 725 21st Street, Northwest, Washington, DC 20052 and Institute for Proteomics Technology and Applications, The George Washington University, 725 21st Street, Northwest, Washington, DC 20052

Annemie Bogaerts
Department of Chemistry, University of Antwerp, Universiteitsplein 1, B-2610 Wilrijk-Antwerp, Belgium

Akos Vertes[a)]
Department of Chemistry, The George Washington University, 725 21st Street, Northwest, Washington, DC 20052 and Institute for Proteomics Technology and Applications, The George Washington University, 725 21st Street, Northwest, Washington, DC 20052

(Received 31 January 2006; accepted 14 June 2006; published online 28 July 2006)

A fluid dynamics model was developed for the ablation of water-rich targets by infrared laser pulses at atmospheric pressure. It incorporates the nonlinear absorption of water and the phase explosion due to superheating. The simulation results show that due to two different phase transition mechanisms, the first, slower plume expansion is followed by a vigorous accelerated expansion. The calculated time evolution of the shock front agrees well with the experimental observations. This model sheds new light on the effect of phase explosion on laser ablation dynamics, and it is relevant for the preparative, analytical, and medical applications. © *2006 American Institute of Physics*. [DOI: 10.1063/1.2243961]

Numerous experimental and theoretical investigations of laser ablation in a background gas are aimed at trying to understand the regimes and processes in this strongly nonlinear interaction.[1–7] Meanwhile, laser ablation is used for a growing number of applications, such as pulsed laser deposition for thin film growth,[4] matrix-assisted pulsed laser evaporation (MAPLE) for the growth of organic films,[8] micromachining,[9] nanoparticle synthesis[10] and chemical analysis.[11,12] Specifically, the midinfrared laser ablation of water-rich targets is very useful for preparative, medical,[13] and analytical applications[11] [e.g., atmospheric pressure matrix-assisted laser desorption ionization (AP-MALDI)]. Despite its many uses, the mechanism of midinfrared laser ablation still awaits detailed description.

Recently, Apitz and Vogel have reported fast imaging results on laser ablation of water, liver, and skin utilizing a 50–100 ns pulse length *Q*-switched Er:YAG (yttrium aluminum garnet) laser.[13] They demonstrate that the ablation proceeds through two consecutive stages. Initially, nonequilibrium surface evaporation takes place. This is followed by a phase explosion of a superheated subsurface layer. They point out that this phase explosion is crucial to the material ejection in water-rich target ablation. A fluid dynamics model that incorporates phase explosion, believed to be also common in femtosecond laser ablation,[12] would provide insight into its effect on the plume expansion dynamics.

Therefore, in this letter, we describe a fluid dynamics model of water-rich target ablation with midinfrared laser pulses at atmospheric pressure in the presence of phase explosion. Compared to laser ablation in vacuum, in a background gas the expansion of the ablation plume is a very complex gas-dynamic process. In order to study the effect of the phase explosion considered here, as a first step, we developed a one-dimensional (1D) fluid dynamics model for water ablation into a 1 atm nitrogen background gas. The 1D approach simplifies the equations of fluid dynamics through neglecting the plume expansion in radial directions. In general, as long as the laser spot size is comparable to the plume size, close to the surface normal of the expansion, the quasi-one-dimensional approximation is reasonable for the plume expansion. The inset in Fig. 1 is from Ref. 13, and it shows that during the first ~900 ns the dimensions of the plume and the laser spot size are comparable. The laser spot size in Ref. 13 is ~0.5 mm, and at ~400 ns in the experiment the distance between the shock front measured along the surface normal and the target surface is ~0.6 mm. At ~1 μs, the distance is about twice the laser spot size and another ejec-

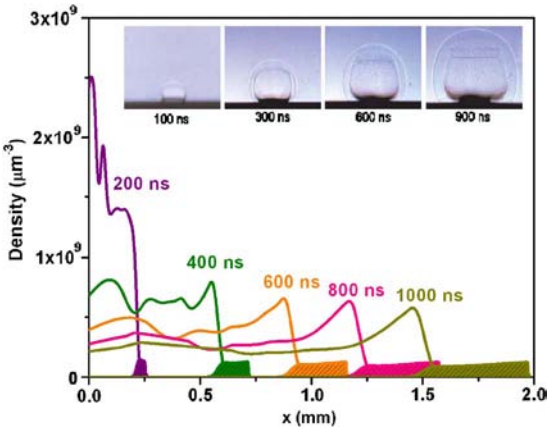

FIG. 1. (Color online) Number density distributions in the water plume for 5.4 J/cm^2 Er:YAG laser ablation of water into 1 atm environment show a high density region close to the shock front and the pileup of background gas at the interface. Solid lines indicate the density of water vapor, whereas filled areas denote the density of background gas. The inset shows the shadowgraph images from the experiments in Ref. 13.

[a)]Electronic mail: vertes@gwu.edu

tion mechanism (a powerful recoil-induced expulsion of liquid water) starts, which is not considered in the model.

The model for condensed phase energy deposition in laser-water interaction is based on the heat transport equation with a penetrating source, i.e., the laser heating of water, the heat conduction, and the evaporation at the water-vapor interface.[14] These processes can be captured on a macroscopic scale by the heat conduction equation in a moving reference frame attached to the evaporating surface and by the Clausius-Clapeyron equation.[15] The heat transport equation is given below:

$$c_p\rho\left[\frac{\partial T(t,x)}{\partial t} - u(t)\frac{\partial T(t,x)}{\partial x}\right] = \frac{\partial}{\partial x}\lambda\frac{\partial T(t,x)}{\partial x} + (1-R)\alpha I(t)\exp(-\alpha x). \quad (1)$$

Here x is the coordinate along the normal to the target surface. In Eq. (1), the target properties C_p, λ, R, ρ, α, and T are the specific heat capacity, the thermal conductivity, the surface reflectivity, the mass density, the optical absorption coefficient at the laser wavelength, and the temperature, respectively. The surface recedes with $u(t)$ velocity and the laser irradiance at the target surface is $I(t)$.

While for Q-switched (nanosecond) laser pulses such a simple model is justified,[15] in the modeling of infrared laser-water interaction, we have to consider three additional factors. First, the dynamic changes in the absorption coefficient of water must be taken into account because the effective absorption coefficient changes up to an order of magnitude as a function of energy per volume deposited at different depths.[16] In the simulation code, the absorption coefficient is initially provided at room temperature, and the energy deposited into a cell during a time step is used to evaluate the nonlinear absorption coefficient for the next time step.

Second, the mass density and the specific heat capacity of water are functions of temperature and can be obtained by the interpolation of tabulated values.[17] Finally, for the experimental fluence range (a few J/cm^2), the rate of energy deposition into the target is high enough to superheat the liquid to the spinodal decomposition temperature. At this temperature phase explosion occurs and a significant volume of the target abruptly transforms from superheated liquid into a mixture of liquid droplets and vapor. This mixture is then ejected from the target.

Perpendicular to the target surface, in the x direction, the 1D plume expansion dynamics can be described by the equations for the conservation of mass, momentum, and energy as well as vapor transport for a binary mixture as follows:[15]

$$\frac{\partial \rho_t}{\partial t} = -\frac{\partial \rho_t \nu}{\partial x}, \quad (2)$$

$$\frac{\partial \rho_\nu}{\partial t} = -\frac{\partial \rho_\nu \nu}{\partial x} + \frac{\partial}{\partial x}\left(\rho_t D_{ab}\frac{\partial}{\partial x}\omega_\nu\right), \quad (3)$$

$$\frac{\partial \rho_t \nu}{\partial t} = -\frac{\partial}{\partial x}\left(\rho_t \nu^2 + P + \frac{\partial}{\partial x}\tau_{xx}\right), \quad (4)$$

$$\frac{\partial}{\partial t}\left[\rho_t\left(U + \frac{1}{2}\nu^2\right)\right] = -\frac{\partial}{\partial x}\left[\rho_t\left(U + \frac{1}{2}\nu^2\right)\nu + P\nu\right] - \frac{\partial}{\partial x}(q + \nu\tau_{xx}) + \alpha_\nu I(t). \quad (5)$$

The definition of the variables in these equations is given in Ref. 15. α_v stands for the highly density dependent light absorption coefficient in the vapor phase.

The 1D calculation is performed simultaneously on two domains, the target domain and the plume domain, each containing a few thousand discrete cells. Numerically, Eq. (1) is solved with a second-order central difference method, and Eqs. (2)–(5) are solved with the combination of the first-order Godunov method (for the convective terms) and a first-order central difference method (for the diffusion, viscosity, and thermal conduction terms).[15] The boundary conditions for the heat conduction and plume expansion equations in the absence of phase explosion (i.e., before and after the phase explosion) are treated the same way as in Ref. 15. The Knudsen layer description is applied to the evaporation process, and the Hertz-Knudsen equation is used to include the back flux to the target surface after the evaporation ceases.

During the phase explosion process, however, the boundary conditions are modified. Due to heat loss through the evaporation process at the surface and as a result of the nonlinear absorption of the laser light in the target, the temperature in the subsurface region can exceed the surface values. Some time after the laser-water interaction starts, a cell beneath the surface reaches a local temperature equal to or higher than $\sim 0.9T_c$ (T_c is the critical temperature). Reaching this spinodal decomposition temperature results in a phase explosion.[5] The liquid-vapor interface at this moment is instantaneously shifted to the location of this cell. From this cell toward the bulk of the target, the temperature gradually decreases from $0.9T_c$ to room temperature and Eq. (1) can be applied to describe the laser target interaction. On the other side of this cell, however, the liquid layer is converted into vapor (phase explosion) and it becomes part of the plume calculation domain. At this point, the temperatures in these cells are directly adopted for the plume domain. After the phase explosion, the algorithm returns to solve the heat conduction and plume expansion equations as discussed above.

Calculations were carried out for the ablation of water by Q-switched Er:YAG laser pulses ($\lambda = 2.94$ μm, $\tau = 70$ ns) at various fluence levels below and above the onset of phase explosion. For the first 1 μs of plume expansion following a 5.4 J/cm^2 laser pulse, time progression of the density distributions is shown in Fig. 1. The formation of a shock front at the contact between the expanding plume and the background gas manifests in steep plume density gradients. The figure also shows the pileup effect in the ambient gas and the elevated plume density near the shock front. At the early stage of plume expansion, the separation between the vapor and the ambient gas is distinct (see the vertical drop in the plume density in Fig. 1); i.e., the contact layer is very thin. But at later stages, due to the binary diffusion process the contact layer becomes thicker, and the vapor and the ambient gas are mixed together.

To quantitatively assess the validity of the predicted dynamics we turn to a comparison with experimental data. Figure 2 presents the measured[13] and our calculated shock front positions $R(t)$ versus time. For the ablation of water by a

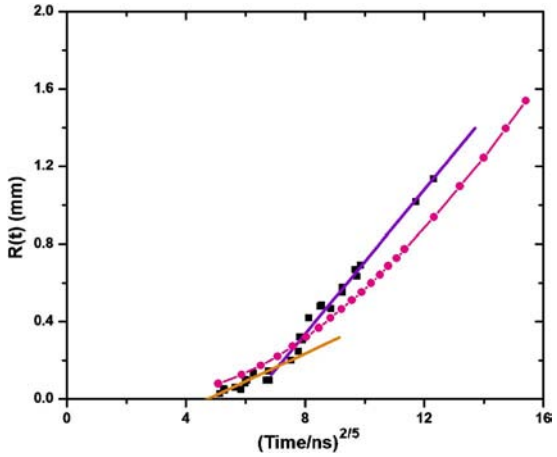

FIG. 2. (Color online) Comparison of experimental water ablation data (Ref. 13) (■) for 5.4 J/cm^2 laser fluence with fluid dynamics calculations including phase explosion (●) and with similarity modeling of two consecutive energy deposition steps (solid lines).

Q-switched Er:YAG laser pulse ($\lambda=2.94$ μm, $\tau=70$ ns) using a moderate fluence (e.g., 5.4 J/cm^2), fast imaging showed that the position of the shock front as a function of time, has a first, slower expansion phase followed by a more vigorous accelerated expansion phase. Rescaling the data in the $t^{2/5}$ variable reveals two distinct slopes corresponding to the two expansion stages (see Fig. 2). These two stages are thought to correspond to fast surface evaporation and to phase explosion.

Comparison of the experimental shock front displacements with our fluid dynamics simulation for the same parameters shows reasonable agreement. Indeed, the calculated slopes during the surface evaporation phase (short times) and the phase explosion phase (long times) accurately follow the experimental values. This is an indication that the energy deposition and redistribution are accurately reflected in the model. The absolute values of the shock front position at long times, however, are underestimated by the model. This might be related to differences between the definition of the shock front position in the experiments and in the calculations, and to the deviation of 1D simulation from three-dimensional (3D) plume expansion. It should also be pointed out that the layer which experiences the phase explosion and has a high number density is not transparent to the laser pulse, and the laser energy absorbed by this layer has a nontrivial effect on the plume expansion dynamics.

To evaluate the relative contribution of the two energy deposition mechanisms, Taylor's 3D similarity theory of shock front displacement is applied. The shock front position can be given as follows:[18]

$$R(t) = S(\gamma)\rho_b^{-1/5}E^{1/5}t^{2/5}.$$

Here $S(\gamma)$ is a weak function of the specific heat ratio of the background gas, γ, ρ_b is the background gas density, and E is the deposited energy. From the ratio of the slopes for the two phases of the plume expansion obtained from the experimental data, s, one can determine the ratio of energies for the surface E_s and volume, E_v, processes: $s=(1+E_v/E_s)^{1/5}$. The deposited laser pulse energy, $E=E_v+E_s$, drives both the surface and volume processes. From the fitted curves in Fig. 2, the slope ratio is $s=2.57$; thus, the ratio of the two energies is $E_v/E_s=111$. One can conclude that the overwhelming majority of the deposited energy is utilized in the volume process. In particular, of the 5.4 J/cm^2 laser fluence only 0.05 J/cm^2 drives the surface evaporation, whereas the remaining 5.35 J/cm^2 is used for the volume process (i.e., phase explosion). During the early stage of laser ablation, close to the expansion axis the plume front displacement is smaller than the laser spot size; thus, the plume expansion is quasi-one-dimensional. It should be pointed out that the current 1D fluid dynamics model cannot predict the water ablation and the plume expansion dynamics at later stages (e.g., at times later than 1 μs) because at later stages of the ablation the two-dimensional plume expansion becomes more noticeable and the recoil-induced material expulsion plays an important role for material transport into the plume.

In summary, we have developed a one-dimensional fluid dynamics model for water-rich target ablation by midinfrared laser pulses that can predict the shock front displacement during plume expansion. The comparison between the experimental and calculated plume shock front positions confirmed the importance of including these effects into the model. The model contributes to the understanding of phase explosion and plume expansion dynamics in water-rich target ablation, and is useful for analytical (AP-MALDI), preparative (MAPLE), and medical (surgery) applications.

The authors are grateful for the insightful comments and for sharing of at the time unpublished data by A. Vogel. This research was supported by the U.S. Department of Energy (DE-FG02-01ER15129), by the W. M. Keck Foundation (041904), by the Flemish Fund for Scientific Research (FWO), and by a bilateral project between Flanders and the P. R. of China. Two of the authors (A.B. and A.V.) are grateful for the Academy Award Fellowship of the Royal Flemish Academy of Belgium for Science and the Arts.

[1] M. Von Allmen, *Laser Beam Interactions with Materials* (Springer, Heidelberg, 1987), Chap. 6.
[2] S. S. Harilal, C. V. Bindhu, V. P. N. Nampoori, and C. P. G. Vallabhan, Appl. Phys. Lett. **72**, 167 (1998).
[3] J. H. Yoo, S. H. Jeong, X. L. Mao, R. Greif, and R. E. Russo, Appl. Phys. Lett. **76**, 783 (2000).
[4] H. Kim, J. S. Horwitz, G. P. Kushto, Z. H. Kafafi, and D. B. Chrisey, Appl. Phys. Lett. **79**, 284 (2001).
[5] Q. M. Lu, S. S. Mao, X. L. Mao, and R. E. Russo, Appl. Phys. Lett. **80**, 3072 (2002).
[6] A. Bogaerts, Z. Y. Chen, R. Gijbels, and A. Vertes, Spectrochim. Acta, Part B **58**, 1867 (2003).
[7] T. Orii, M. Kirasawa, and T. Seto, Appl. Phys. Lett. **83**, 3395 (2003).
[8] A. Pique, R. A. McGill, D. B. Chrisey, D. Leonhardt, T. E. Mslna, B. J. Spargo, J. H. Callahan, R. W. Vachet, R. Chung, and M. A. Bucaro, Thin Solid Films **355/356**, 536 (1999).
[9] J. Li and G. K. Ananthasuresh, J. Micromech. Microeng. **11**, 38 (2001).
[10] D. B. Geohegan, A. A. Puretzky, G. Duscher, and S. J. Pennycook, Appl. Phys. Lett. **72**, 2987 (1998).
[11] V. V. Laiko, N. I. Taranenko, V. D. Berkout, M. A. Yakshin, C. R. Prasad, H. S. Lee, and V. M. Doroshenko, J. Am. Soc. Mass Spectrom. **13**, 354 (2002).
[12] R. E. Russo, X. L. Mao, and S. S. Mao, Anal. Chem. **74**, 70A (2002).
[13] I. Apitz and A. Vogel, Appl. Phys. A: Mater. Sci. Process. **A81**, 329 (2005).
[14] H. C. Le, D. E. Zeitoun, J. D. Parisse, M. Sentis, and W. Marine, Phys. Rev. E **62**, 4152 (2000).
[15] Z. Y. Chen and A. Bogaerts, J. Appl. Phys. **97**, 063305 (2005).
[16] R. K. Shori, A. A. Walston, O. M. Stafsudd, D. Fried, and J. T. Walsh, Jr., IEEE J. Quantum Electron. **7**, 959 (2001).
[17] W. Wagner and A. Pruß, J. Phys. Chem. Ref. Data **31**, 387 (2002).
[18] G. Taylor, Proc. R. Soc. London, Ser. A **201**, 159 (1950).